Synthesis and Characterization of Pyrogallol–Formaldehyde Nano Resin and Its Usage as an Adsorbent

ARTICLE *in* JOURNAL OF CHEMICAL & ENGINEERING DATA · SEPTEMBER 2012

Impact Factor: 2.04 · DOI: 10.1021/je300582y

3 AUTHORS:

Mustafa Can
Sakarya University
15 PUBLICATIONS **58** CITATIONS
SEE PROFILE

Emrah Bulut
Sakarya University
14 PUBLICATIONS **402** CITATIONS
SEE PROFILE

Mahmut Ozacar
Sakarya University
52 PUBLICATIONS **2,377** CITATIONS
SEE PROFILE

Journal of chemical & engineering data

Article

pubs.acs.org/jced

Synthesis and Characterization of Pyrogallol-Formaldehyde Nano Resin and Its Usage as an Adsorbent

Mustafa Can,*[,†,§] Emrah Bulut,[‡] and Mahmut Özacar[‡]

[†]Institute of Sciences and Technology and [‡]Department of Chemistry, Sakarya University, 54187 Sakarya, Turkey

ABSTRACT: A pyrogallol (PG) and formaldehyde condensation reaction was carried out under alkaline conditions to prepare the pyrogallol−formaldehyde resol resin (PGNR). Polymerization was performed to establish the nano resin formation. Obtained nano resin was used as an adsorbent for recovery of rhodium(III) ions from chloride-containing solutions. This kind of recovery was very simple and useful for generating little secondary wastes. The interaction of adsorption also was investigated: The proposed adsorption of the aquachlororhodium(III) species mostly takes place via a ligand exchange mechanism. PGNR and Rh-adsorbed PGNR were characterized by scanning electron microscopy, energy-dispersive spectrometry, X-ray diffraction spectroscopy, and Fourier transform infrared−attenuated total reflection spectroscopy. By utilizing such characteristics of polyphenol resin, PGNR can be applied to recover Rh(III) efficiently and simply with low cost.

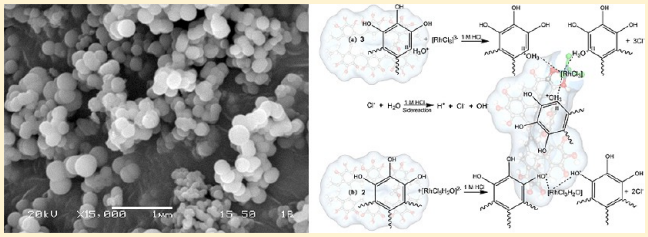

1. INTRODUCTION

Tannins represent secondary metabolites whose main role in plants is primarily defensive. Tannin and its derivates gallic acid and pyrogallol are an excellent resource for replacing petroleum-derived phenolic compounds.[1] Gallic acid consists of aromatic ring bearing carboxyl group and three adjacent hydroxyl groups. These carboxyl groups, besides deactivating the molecule toward formaldehyde, limit the amount of methylol formations to two per molecule, which leads to linear molecules.[2] Pyrogallol (PG) can be obtained from hydrolyzable tannins by two consecutive transformations.[3] Comparing to gallic acid formaldehyde polymerization reaction, PG and formaldehyde react extremely quickly, thus attaining the resin's particle nano diameter.

Conventional syntheses of polyphenol resins are classified into chemical and enzymatic methods.[2] In the chemical methods, phenol reacts with formaldehyde in acidic or alkaline media, forming novolac or resol resins, respectively.[4] Acid-catalyzed resins behave like thermoplastics. Alkaline-catalyzed phenolic resins are considered to be thermosetting resins.[5] These polymers characteristically possess excellent mechanical strength, durability to chemicals, and insulation properties. Thus they have applications in the automobile, wood panel, aerospace, and electrical industries.[6] Adam and Holmes[7] first demonstrated the capacity of organic anion and cation exchange type resins to exchange cations on the very weakly dissociating phenolic groups.[8,9] These can be used for isolating and separating rare alkali metals,[10] actinide,[11−14] and precious metals.[15,16]

Increasing demand for the platinum group metals (PGMs) for the production of catalysts and in related industries, combined with the limited resources available, has led to the increasing interest in the recovery of these strategic elements.[17] Only a few studies have been carried out on the separation of PGMs using tannin derivatives.[18−21] Nevertheless, the successful adsorption and separation of Rh(III) are not achieved. Various types of adsorbents have been studied. Uheida et al.[22] have reported that Fe_3O_4 nanoparticles show high affinity for Rh(III) ions and predominantly adsorb Rh(III) ions in the coexistence of Pd(II) and Pt(IV) ions. The adsorption capacity was determined to be 14.82 mg of Rh(III)/g of Fe_3O_4. Turner et al.[23] reported 5 mg·L^{-1} Rh(III) adsorption capacity onto estuarine sediment. A Fe(III)-templated oxine type of chemically modified chitosan was prepared to examine the adsorptive separation of Rh(III) from chloride media containing S(II). The maximum adsorption capacity was evaluated to be 97.91 mg of Rh(III)/g of dry adsorbent.[24] In addition, Goto et al.[25] studied the adsorption of Rh(III) using chemically activated carbon pellets. They achieved an adsorption capacity for Rh(III) 15 mg/g of dry activated carbon pellets. The reduction in size of the particles results in an extremely large surface area-to-volume ratio and increased surface reactivity, which also means increased metal ion adsorption capacity.[26]

PG consists of an aromatic ring bearing three adjacent hydroxyl groups (positions 1, 2, and 3), leaving three free sites on the ring. Reactivity considerations show that the hydroxyl functions enhance the reactivity of positions 4 and 6. The remaining position (5) would have the same degree of activation as phenol (Figure 1a). These three possible reactive sites permit the eventual formation of a tridimensional network during polymerization as in the case of phenol. Thus, we decided to study the reactivity of PG in the synthesis of PGNR.[17]

Received: May 28, 2012
Accepted: September 10, 2012
Published: September 18, 2012

dx.doi.org/10.1021/je300582y | *J. Chem. Eng. Data* 2012, 57, 2710−2717

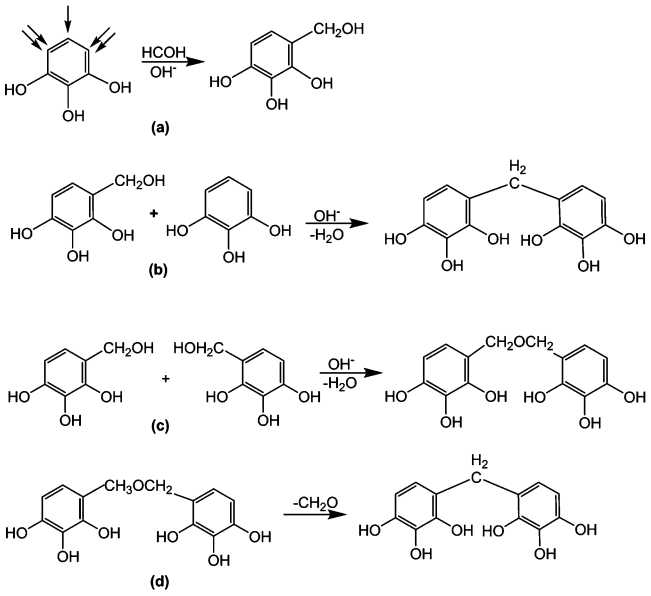

Figure 1. Reaction of PG with formaldehyde. (a) Methylation reaction of PG; (b) formation of methylene bridges in PGNR; (c) formation of dimethyl ether bridges in PGNR; (d) transformation of dimethyl ether bridges to methylene bridges.

Fourier infrared (FT-IR) spectroscopy is a powerful analytical method for monitoring the curing process. Valuable qualitative and semiquantitative information, for example, on the type of reaction, can be obtained from IR studies. In particular, the appearance of the hydroxyl group, methylol group, and dimethylene ether bridges can be easily monitored.[27] Scanning electron microscopy (SEM) has been used to show the particle size and morphology of these resins. Energy-dispersive spectroscopy (EDS) analysis was performed to determine elemental distribution for a scanning surface in samples.[28]

Adsorption studies using polyphenols are already known. In addition phenolic resins that have been produced from various phenolics have an extensive literature base. However, the majority of these studies focus on base metal adsorption. Also, as far as we could find in recent reports, an adsorption study with the resin derived from pyrogallol has not been reported. On the other hand, particle size is one of the most important factors that increases the surface area. Having good PGNR nanosize particles is important in this regard. Therefore we decided to use PGNR as an adsorbent for Rh(III) adsorption. One of the other factors that increases adsorption is functional groups of resin structure. Having the ability to create quinone structures of PGNR is also an indication of the ability of metal reduction. Further, the π sites in the carbons of the pyrogallol phenol can be playing an important role in adsorption. According to this model, when the solution was used at a higher pH, a large amount of H_3O^+ was first adsorbed in the π sites. These sites could be the π sites, which are capable of acting as the electron donors (Lewis-type acid) to form a coordination bond with anionic complexes of Rh(III) in which they act as a Lewis-type base.[29] The capability to adsorb from two sites of resin has indicated that PGNR provides efficient capacity and fast kinetics on adsorption.

This study focused on two main areas: first, the investigation of pyrogallol–formaldehyde resol resin (PGNR) formation using several techniques such as FTIR, SEM, EDS, and XRD, and second, interaction characterization of rhodium(III) ions in chloride containing aqueous solutions onto obtained PGNR particles.

2. MATERIALS AND METHODS

2.1. Materials. Pyrogallol was purchased from Alfa Aesar GmbH&Co. $RhCl_3 \cdot 3H_2O$ (containing 38 % Rh), NH_3, HCOH, HNO_3, HCl, NaCl, and NaOH were purchased from Merck Company. Flame atomic absorption spectrometry (FAAS) standard solutions for the determination of Rh were purchased form UltraScientific Company. All other reagents were analytical grade. The aqueous Rh(III) stock solution was prepared from solid $RhCl_3 \cdot 3H_2O$ in 1.0 M HCl. Adsorption experiments were carried out with a change from (20 to 150) $mg \cdot dm^{-3}$ Rh(III) initial concentration.

2.2. Instruments. The contents of Rh(III) in solutions were analyzed by FAAS (Shimadzu 6701F). FT-IR spectral analysis of resins was performed by Shimadzu IRPrestige-21. To determine which bonds formed during the formation of resin, the FT-IR spectra analyses of PG and PGNR were carried out. In addition to describing resin's interaction mechanism with Rh complexes, the FT-IR spectra analyses of PGNR and Rh adsorbed PGNR were performed. The spectra were recorded from (1800 to 700) cm^{-1} (25 scans) on sample. To eliminate moisture and CO_2 interferance, background spectra were recorded before analysis of the samples. Later on, it was corrected by applying IRsolution software's Kubelka–Munk function attenuated total reflection (ATR)-correction function. The Kubelka–Munk theory is generally used for the analysis of diffuse reflectance spectra obtained from weakly absorbing samples. It provides a correlation between reflectance and concentration. The concentration of an absorbing species can be determined using the Kubelka–Munk formula.[30,31] Samples were analyzed using a ceramic light source, KBr/Ge beam splitter, and a deuterated L-alanine triglycine sulfide (DLATGS) detector. DRIFTs bands are stronger than expected absorption from weak IR bands. Compensation by Kubelka–Munk conversion creates a linear relationship for spectral intensity relative to sample concentration.[32] SEM and EDS experiments were carried out on JEOL JSM-6060LV scanning electron microscope operated at 20 kV. The morphology and size of PGNR was investigated using SEM. To show the presence of Rh on the PGNR, EDS analysis was performed. To clarify the interaction mechanism, X-ray diffraction analysis of PGNR measured with RIGAKU D_{max} 2200 at a Cu anode producing Kα radiation (40 kV, 30 mA). The specific surface area of the resin was determined with BET nitrogen adsorption using a Micromeritics Flow Sorb 2300.

2.3. Preparation of PGNR. A solution of PG (40 g, ~0.317 mol) in deionized water (200 mL) and NH_3 solution (20 % w/w, 7 mL) was heated to 70 °C with magnetic stirring. Then formaldehyde (P) (37 % w/w, 50 mL) was added, and the reaction mixture was heated at this temperature.[17] To achieve resistance under adsorption conditions (1 M HCl), different curing times were used. Pre-experiments showed that 1 h was enough time for resistance. At the end of the production of GAR, the amount of formaldehyde was determined by iodometrically as 1.26 per thousand. This value does not exceed the appropriate limit of 1 %.[2]After the resulting liquid containing the precipitate was filtered through filter paper the obtained insoluble PGNR was washed with distilled water to make formaldehyde free resin.[1] Then the filtered precipitate was dried at 80 °C.

2.4. Adsorption Studies. Adsorption experiments were carried out by agitating 0.2 g of PGNR with 50 mL of Rh(III) ion solution in 1 M HCl concentration at 20 °C. Initial Rh(III) concentrations were selected at the desired concentration for 4 h. All adsorption experiments were carried out in a standard and strictly adhered to a batchwise system. At the end of the adsorption period, 15 mL samples were centrifuged, and the solutions were filtered through a 0.45 μm Milipore filter paper to avoid any solid particle in the aqueous phase. Samples were measured using FAAS. All of the adsorption tests were performed at least twice so as to avoid wrong interpretation owing to any experimental errors.

FAAS are calibrated using (0, 4, 12, and 20) ppm standard solution containing 1 M HCl. The amount of adsorbed Rh(III) was calculated from the concentrations in solutions before and after the adsorption process. Results used the average of three scans for each sample.

3. RESULTS AND DISCUSSION

3.1. Preparation of PGNR. Alkaline-catalyzed (resol) PGNR was prepared similar to phenol-formaldehyde resins. Resol resins of phenol/formaldehyde (F/P) had a molar ratio generally higher than 1.[33] Studies in the literature have shown that an optimal resol molar ratio for PG is 2.1.[17] PG is soluble in water; the solubility of PGNR was measured to achieve resistance under adsorption conditions. Different curing times have been carried out. Pre-experiments (not shown here) showed that 1 h is enough time for resistance.

There have been two steps leading to the formation of PGNR: methylolation and condensation reactions as shown in the Figure 1. The first step, methylation, completes an electrophilic aromatic substitution reaction, and consequently, the products obtained will be substituted in *ortho* and *para* positions (Figure 1a). The second step consists of a condensation reaction. In this reaction, two mechanisms involve a hydroxymethyl group with either a PG forming methylene linkage (Figure 1b) or a hydroxymethyl group forming dimethyl ether linkage (Figure 1c), releasing a water molecule. Although the dimethyl ether linkage transforms into a methylene linkage by the application of heat (Figure 1d), a little ether linkage still remains in the resin structure.[34] This confirms PGNR's FT-IR spectra. These mono- or polynuclear hydroxymethyl phenols, which were stable at room temperature, are transformed into three-dimensional, cross-linked, insoluble, and infusible polymers by the application of heat.[33]

The PGNR structure can be seen from Figure 2. Since PG includes three free sites for the formation of methylene and dimethyl ether bridges, a three-dimensional resin structure will be formed. Due to insoluble cross-linked structure of GAR formed by the reaction of GA with formaldehyde, a perfect adsorbent property has been seen for the adsorption of PGMs and unwanted heavy metal containing compounds from aqueous solutions.[17,35]

3.2. FT-IR Spectroscopy Studies. Figure 3 represents the FTIR-ATR normalized spectra of PG, PGNR, and Rh adsorbed PGNR. The main bands and their assignments in PG are as follows: stretching vibrations of the aromatic ring ν(C−C)/ν(C═C) at (1620, 1518, and 1483) cm^{-1},[36] stretching vibrations of the phenolic group ν(C−OH) at (1314, 1287, 1242, and 995) cm^{-1},[27] in-plane bending vibrations of the phenolic group d_{ip}(O−H) at (1483, 1362, 1287, 1186, and 1156) cm^{-1}, out-of-plane bending vibrations of the phenolic group d_{ip}(O−H) at 680 cm^{-1}, and torsional vibrations of

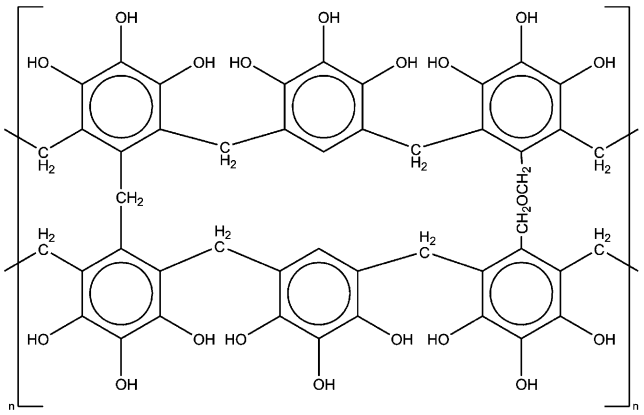

Figure 2. Proposed structure of PGNR.

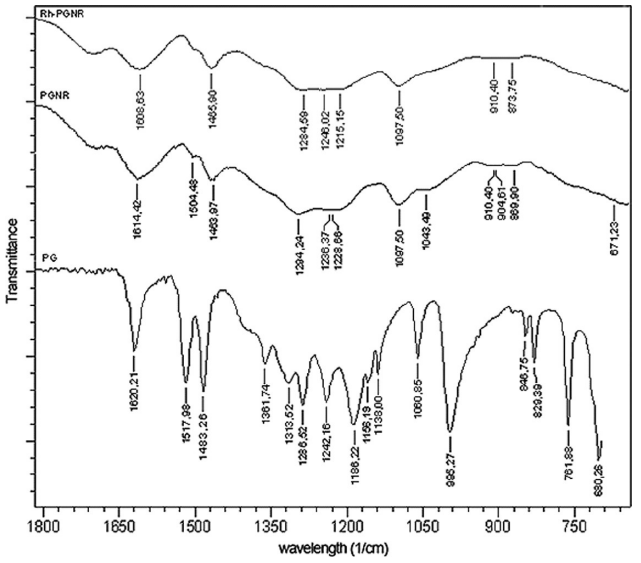

Figure 3. FTIR spectra of PG, PGNR, and Rh adsorbed PGNR.

benzene t(CH) at 762 cm^{-1}.[27,37] Assigned spectra peaks are presented in Table 1, and here the contributions to IR intensities and frequencies were written highest to lowest.

The formation of PGNR leads to obvious changes in FTIR spectra: the new structure consisting of a large molecule that is attenuated to many peaks. Due to participationg in the chemical reaction during the formation of GAR, the stretching vibrations of benzene group's carbons corresponding to (1620 and 1518) cm^{-1} regions showed a decrease and slightly shifted to 1607 cm^{-1}. The deformation vibrations of the C−H bond in benzene rings at (1138, 829, and 762) cm^{-1} completely disappeared due to polymerization.[38] The complete disappearance of the bands at (1362, 1314, 1287, 1242, and 1186) cm^{-1} peaks in PG are combined to create broad peaks at (1229 to 1236) cm^{-1}. The band intensity at 1287 cm^{-1} is reduced and shifted to 1294 cm^{-1} in the spectrum of the PGNR. This situation may be attributed to a combination of in-plane deformation and asymmetric stretch of phenolic −OH groups.[33] Also, the formation of dimethyl ether bridges (−CH$_2$−O−CH$_2$−) appeared at 1098 cm^{-1}.[27,33] Since the most characteristic absorption of aliphatic ethers is a strong band in the 1150−1085 cm^{-1} region due to asymmetrical C−O−C stretching, this band usually occurs near 1125 cm^{-1}.[1,27,33,39] Peaks at (1061, 995, and 847) cm^{-1} in PG

dx.doi.org/10.1021/je300582y | J. Chem. Eng. Data 2012, 57, 2710−2717

Table 1. Assignment of Absorption Bands of the PG

wave no.[a] (cm^{-1})	assignment[b]	nature
1620	ν(CC)	benzene
1518	ν(CC), ν(C−O)	benzene, methylol
1483	ν(CC), d_{ip}(CH), d_{ip}(O−H)	benzene, benzene, benzene
1362	d_{ip}(O−H), ν(CC), d_{ip}(CH)	phenolic, benzene, benzene
1314	ν(C−O), ν(CC)	methylol, benzene
1287	ν(C−O), d_{ip}(O−H)	phenolic, phenolic
1242	d_{ip}(CH), ν(C−O), ν(CC)	benzene, methylol, benzene
1186	d_{ip}(O−H), ν(CC), d_{ip}(CH)	phenolic, benzene, benzene
1156	d_{ip}(O−H), ν(CC), d_{ip}(CH), ν(C−O)	phenolic, benzene, benzene, methylol
1138	d_{ip}(CH), ν(CC)	benzene
1061	ν(C═C), d_{ip}(CH)	benzene
995	ν(C−O), ν(CC)	methylol, benzene
847	d_{op}(C−H), ν(C−O)	benzene, methylol
829	d_{ip}(CH)	benzene
762	t(C−H)	benzene
680	d_{ip}(O−H)	phenolic

[a]Estimated uncertainty = ± 1 cm^{-1}. [b]ν = stretching, d = deformation, ip = in plane, op = out of plane, t = torsion. The contributions to IR intensities and frequencies were written highest to lowest.

Table 2. FTIR Spectral Properties of PGNR before and after Sorption of Rh(III)

	absorption bands[a] (cm^{-1})		
IR peak	before sorption	after Rh sorption	assignments[b]
1	1614	1609	ν(CC), d_{ip}(CH) benzene
2	1505	disappear	ν(CC) methylene and benzene, d_{ip}(CH) benzene
3	1464	1466	ν(CO) phenolic, ν(CC) methylene and benzene
4	1294	1285	d_{ip}(O−H) phenolic, ν(CO) phenolic
5	1237	1246	ν(CC) benzene, ν(CO) phenolic
6	1229	1215	ν(CC), d_{ip}(CH) benzene, ν(CO) phenolic
7	1098	1098	ν(COC) ether
8	1044	disappear	d_{ip}(O−H)
9	910	910	d_{op}(O−H) phenolic, and ether bridge
10	905	disappear	d_{op}(O−H) phenolic, and ether bridge
11	870	874	d_{op}(C−H) methylene bridge
12	671	disappear	d_{op}(O−H) phenolic

[a]Estimated uncertainty = ± 1 cm^{-1}. [b]ν = stretching, d = deformation, ip = in plane, op = out of plane, t = torsion.

combined to 1044 cm^{-1} in PGNR. This corresponded to single bond C−O stretching vibrations of $-CH_2OH$ group. The (910, 905, 870, and 671) cm^{-1} peaks belong to the C−H and O−H out-of-plane vibrations.[40] The peak intensities at (1483, 1362, 1287, 1186, and 1156) cm^{-1} are reduced and shifted to (1505 and 1464) cm^{-1} creating broad peaks due to the formation of methylene bridges ($-CH_2-$).[33]

The (1518, 1362, 1314, 1287, 1186, and 1156) cm^{-1} peaks (Table 1) are mostly representing d_{ip}(O−H) of phenolic groups.[33,38,41] Some of them completely disappear; some of them still remain but are combined with other peaks in PGNR spectra. Despite the use of phenolic OH groups of during the formation of resin, (1464, 1294, 1237, and 1215) cm^{-1} peaks (Table 2) indicate that PGNR contains OH groups. These groups can interact with PGM ions, and this clearly seen in the GAR-Rh spectrum (Figure 3).

The out of plane deformation vibrations of the (C−H) bond in the benzene rings give absorption bands in the 847 cm^{-1}. This group disappears during the process of polymerization; therefore, these behaviors are attributed to the difficulty of phenolic ring deformation when it is highly cross-linked.[41−43] At the same region a small peak appears due to the formation of a methylene bridge's (C−H) bond out-of-plane deformation. The functional groups before and after adsorption on PGNR and the corresponding infrared absorption bands are shown in Table 2. The spectra display various absorption peaks, confirming the structure of PGNR.

When the spectra of Rh adsorbed PGNR were compared with the spectrum of the PGNR, the small peak series at (1294 and 1044) cm^{-1} are combined and reduced peak intensities, because of PGNR-Rh complex formation between Rh and some phenolic groups of PGNR.[37,38,44] In general it may be argued that the degree of adsorption caused a proportional reduction of the degree of freedom.[1,27] The possible interaction between rhodium chloro aqua complexes and PGNR is represented in Figure 4.

Adsorption Studies. All Rh(III) species in Cl^- ion containing aqueous solutions does not interact with PGNR particles. The adsorption capacity and adsorption rate of rhodium onto the PGNR particles depend on the distribution of Rh(III) species because the adsorbabilities of species differ from each other due to their different chemical structures.[4] Rhodium(III) forms octahedral complexes with halides that present a complex speciation in chloride solutions due to the formation of a variety of aqua/chloro complexes. The formation of the aqua containing complexes depends on the chloride concentration, temperature, time after preparation, and the pH of the solution. $RhCl_6^{3-}$ undergoes stepwise aquation until the stable $RhCl_3(H_2O)_3$ complex is formed.[45] These aqua chloro complexes may also undergo hydrolysis time after preparation at 1 M H^+ concentration. This reaction, which is pH-dependent, may lead to association or precipitation.[46] Thus, the structure of rhodium complexes becomes relatively larger, and this case makes adsorption harder than with chloro rhodium species. To avoid this negative influence, the experiments can be completed at a higher pH.[25,47,48] In addition, to eliminate the water molecule effect, concentrated Cl^- ions should be used. In this way, relatively small complexes should be involved. At higher HCl concentrations, PGNR particles begin to dissolve. Moreover, too high HCl concentrations change the PGNR crystallinity and thus reduce the probability that the acid will change the shape of the adsorption internal sites.[49] Given all these facts, the most appropriate media for Rh(III) adsorption is aqueous solution containing 1 M HCl. Adsorption experiments were therefore performed in 1 M HCl containing solutions. In these conditions, Rh(III) exists in a $[RhCl_6]^{3-}/[RhCl_5H_20]^{2-} > 1$ concentration ratio.[48,50] Consequently, Rh(III) is the most difficult adsorbent in the platinum group of metals.[25,46]

Figure 5 shows the adsorption capacities of Rh(III) ions at various initial metal concentrations. In all cases the plots form a plateau at higher metal concentrations, which is suggestive of the fact that adsorption has reached out to equilibrium. The adsorption capacity of PGNR particles with respect to Rh(III) were determined as 15.43 $mg{\cdot}g^{-1}$. A Langmiur single layer adsorption capacity of PGNR was found as 59.01 mg of Rh(III)/g (calculations will be presented at a later date). This result shows that GAR particles can be used efficiently for the

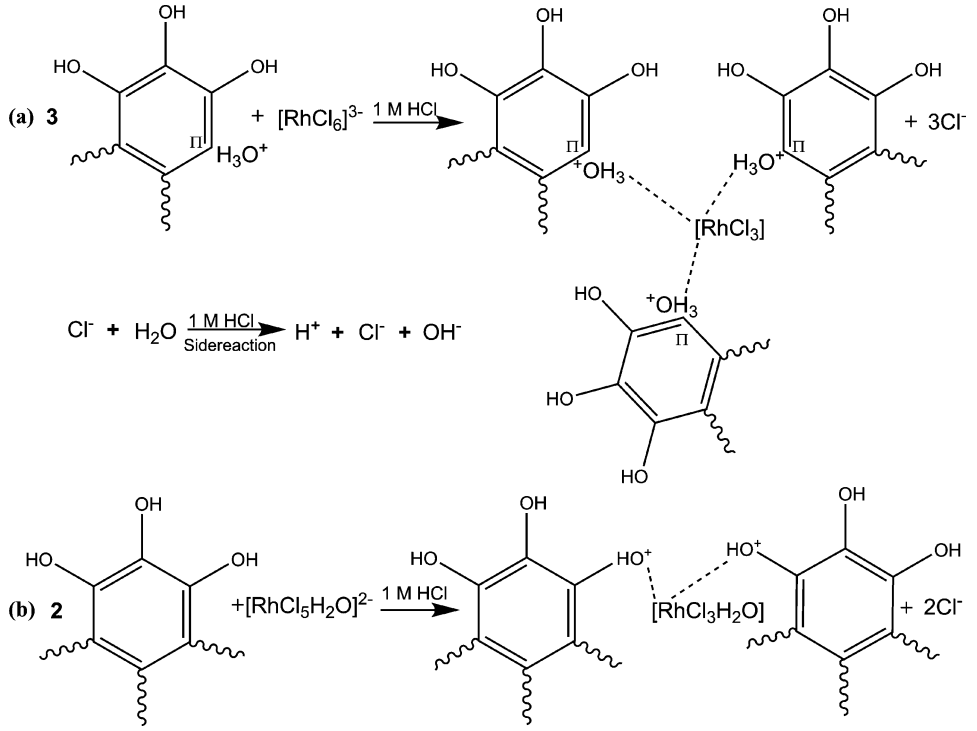

Figure 4. Adsorption mechanism of Rh(III) species: (a) $[RhCl_6]^{3-}$ surface complex formation with protonated π carbons of GAR and (b) $[RhCl_5H_2O]^{2-}$ surface complex formation with phenolic functional groups of GAR.

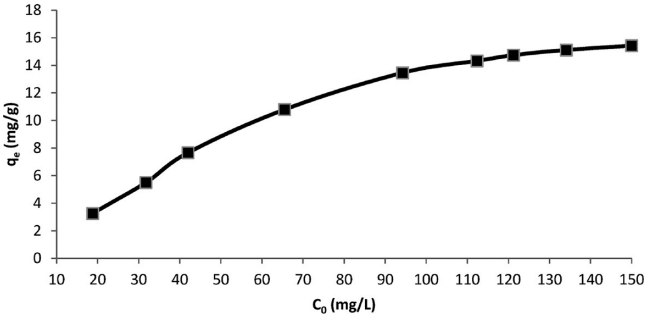

Figure 5. Plots of adsorption capacity vs initial metal concentration (1 g of PGNR, 20 °C, $[H^+]$ = 1, $[Cl^-]$ = 1 M, V = 1000 mL).

removal of Rh(III) when it compared to literature results.[18,25,26,29,18]

3.3. Instrumental Measurements. The SEM image of PGNR is shown in Figure 6, and the EDS pattern of Rh adsorbed PGNR is given in Figure 7. As can be seen in Figure 6, PGNR resin particles have a spherical and uniform structure. The particle size of PGNR is around 250 nm. Such particles which have a very small radius (125 nm) may be necessary to increase the surface area. Therefore, the adsorption capacity will increase. The Branauer–Emmett–Teller (BET) specific surface area of the resin was determined to be 4.01 $m^2 \cdot g^{-1}$ from adsorption–desorption isotherms obtained at the temperature of liquid nitrogen using an automated physisorption instrument. Because PGNR's surface does not contain many pores, the BET surface area measurement gives a relatively small value. On the other hand, big rhodium complexes cannot move into pores of resin where the majority of rhodium adsorbed on the surface may be considered. Thus, the synthesized PGNR have been successfully used for the adsorption of Rh(III) ions. The corresponding EDS spectrum (Figure 7) gives the signals of Rh element, confirming the existence of Rh on the PGNR surface. EDS analysis did not provide us precise information about the metal binding mechanism on the surface, but it also provided us with the ability to make supportive comparisons.

When comparing the amount of Rh(III) and Cl^- ions in EDS spectra (Figure 7), the percentages are respectively 0.71 % and 2.29 % of the surface. The presence of a very small amount of rhodium against chlorine can be explained by Rh(III) complexed with Cl^- ions on the PGNR surface. This shows that the Rh(III) adsorption stage is surface complex formation. XRD pattern results (Figure 8) will help us to make a final decision on this issue.

Adsorption Mechanism. Multiple hydroxyl groups in PGNR are required for the efficient adsorption of rhodium ions.[47] Rh(III) adsorption in chloride containing aqueous solutions is difficult because it has six coordination numbers and formed aqua and hydroxyl containing big chloro aqua rhodade complexes with time. This complex species exists in high pH and at lower chloride concentrations.[25,47,48,50] Rh(III) exists in aqueous chloride solutions as a mixture of $[RhCl_{6-n}(H_2O)_n]^{(3-n)+}$ complexes, and interconversion of these complexes is very slow indeed. The 1 M and above HCl concentrations give low complex species.[48] Adsorption experiments were performed in 1 M HCl containing solutions. In these conditions, Rh(III) exists in a $[RhCl_6]^{3-}/[RhCl_5H_20]^{2-} > 1$ concentration ratio.[48,50] All of this makes Rh(III) the most difficult adsorbent in the platinum group of metals.[25]

Rhodium coordinates with two OH units in PG units of PGNR to form quinons.[51,52] It is known that the addition of Sn(II) chloride to an aqueous solution containing Rh(III) results in the formation of binuclear complexes between Rh and $SnCl^{2-}$, reducing trivalent rhodium to the monovalent state. Since these complexes are more labile than aqua chloro complexes of Rh(III), these complexes have a high affinity to

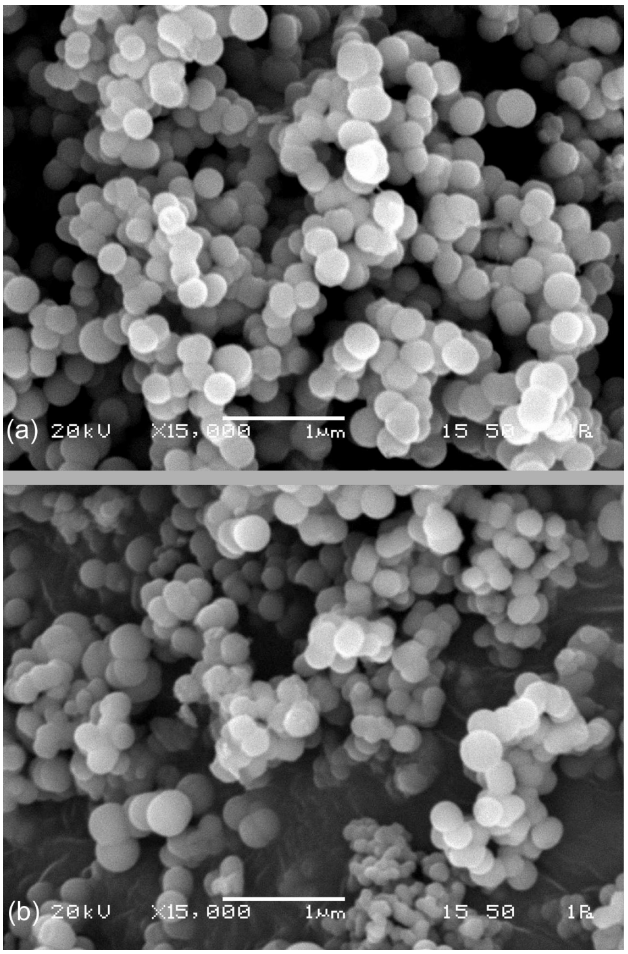

Figure 6. SEM micrograph of adsorbed Rh(III) (a) and natural (b) GAR particles (15000× magnification, 20 kV).

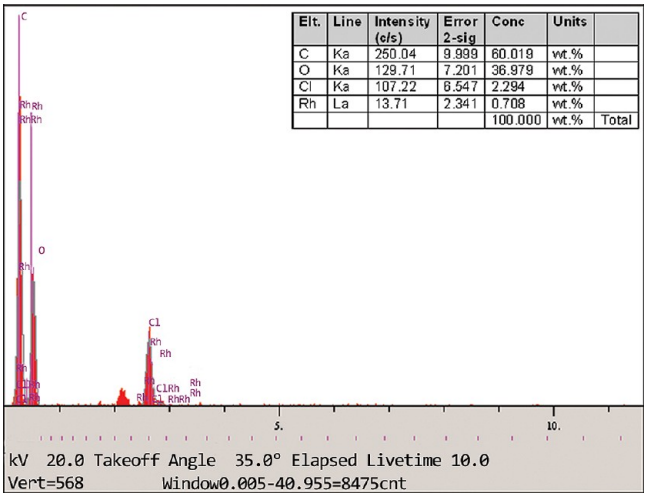

Figure 7. EDS pattern of Rh adsorbed PGNR.

PGNR.[24] The reduction potential of Rh(III) is 0.310 V which is lower than Rh(I)'s 0.600 V. When PGNR's potential of 0.600 V was considered, this potential remains low. This also supports the fact that modification with Sn(II) increases adsorption capacity.

When the redox potentials of phenol derivates are high, they have a lower reduction ability toward the Rh(III) ion.[4]

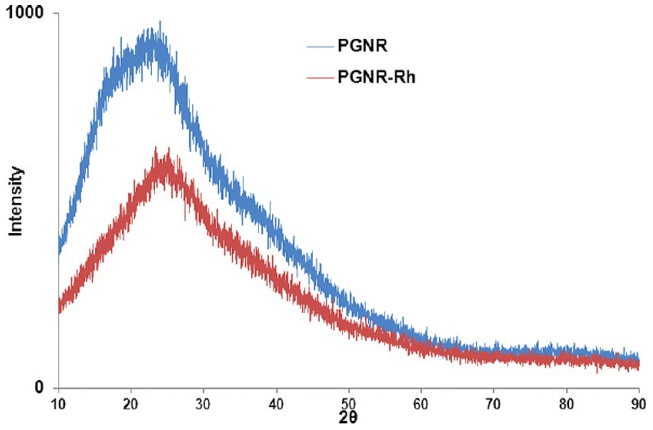

Figure 8. XRD pattern of PGNR before and after Rh(III) adsorption.

Containing an electron-donating substituent such as methylene and a dimethyl ether linkage in PGNR enhances the adsorption of Rh(III) complexes.[4] This situation can be seen at Table 3 for phenol derivatives. Although the PGNR redox potential is not known, it must be lower than PG's 0.713 V. For all that, when considering three-dimensional structures, the adsorption of rhodium complexes was difficult.

Table 3. Redox Potential of Phenol Derivatives

monomer	ORP (mv)[a,b]	ref
catechol	638	4
3-metylcatechol	605	4
4-metylcatechol	595	4
4-ethylcatechol	590	4
m-cresol	710	4
pyrogallol	713	39

[a]Estimated uncertainty = ± 3 mV. [b]ORP: oxidation−reduction potential.

The PGNR redox potential is around 600 mV.[4,52] Under the conditions of pH 0 and pCl 0, as mentioned before, the predominant species of Rh(III) have a $[RhCl_6]^{3-}/[RhCl_5H_2O]^{2-} > 1$ concentration ratio.[48,50] When compared to the reduction potential of rhodium complexes (310 mV),[48,53] it can be concluded that there has not been Rh(III) reduction. At least catodic and anodic redox potentials must be same or approximately same.[16,54]

In addition to the discussion above, to determine the state of recovered rhodium, XRD analysis used as a convenient method.[55,56] The XRD pattern of PGNR and rhodium adsorbed PGNR are shown in Figure 8. The absence of crystal structure can be clearly seen in diffraction patterns. In other words, there is no metallic rhodium on the surface. Possible adsorption mechanisms were ion exchange and complexation. In the spectra of Rh adsorbed PGNR, when compared to the spectrum of the PGNR shown in Figure 3, the small peak series at (1294 and 1044) cm^{-1} are combined and reduced peak intensities. These peaks represent PGNR-Rh surface complexation as shown in Figure 4.

4. CONCLUSIONS

PG-formaldehyde resol type condensation has been studied. Characterization was performed using FTIR and SEM instruments. PGNR, which are obtained by the condensation reaction between formaldehyde and PG, do not dissolve in

dx.doi.org/10.1021/je300582y | J. Chem. Eng. Data 2012, 57, 2710−2717

water, whereas the PG dissolves in water. The radius of PGNR particles was measured as around 125 nm. It was used as adsorbents for the removal of Rh(III) ions from 1 M HCl solutions. The adsorption capacity of PGNR particles with Rh(III) was determined as 15.43 $mg \cdot g^{-1}$. PGNR particles were used as an adsorbent for the removal of Rh(III) ions from 1 M HCl solutions. Rh(III) species $[RhCl_5H_2O]^{2-}$ and $[RhCl_2(H_2O)_4]^-$ have been adsorbed onto polyphenol resin surface. Complexation as possible adsorption mechanisms was proposed and discussed; meanwhile, the reduction of Rh(III) species to metallic form does not occur in under these conditions. Obtained PGNR was characterized by FTIR spectroscopy before and after adsorption of rhodium metal ions. For the recovery of PGM, the results obtained here show that PGNR particles can be used as an effective adsorbent from aqueous solution.

For the recovery of Rh(III), PGNR adsorbent has been quite an effective way to achieve a series of unit operations (extraction, reduction, adsorption, solid−liquid separation) simultaneously onto the PGNR, and there was a little secondary waste (nonadditives for reduction and precipitation). Therefore, this system shows good promise as a recovery method for PGMs. It is expected that not only the efficient Rh(III) adsorption but also the separation from the mixture of metal ions will be possible using PGNR particles by controlling the solution composition (pH, pCl, ionic strength, and distribution of PGM species). However, by utilizing such characteristics of polyphenol resin particles, it is expected that they can be applied to recover Rh(III) efficiently and simply with low cost.

AUTHOR INFORMATION

Corresponding Author

*Tel.: 0264 295 60 41. Mobile phone: 0505 253 21 00. Fax: 0264 295 59 50. E-mail: mstfacan@gmail.com.

Present Address

[§]Ministry of Education, Adapazari Imam Hatip School, 54100 Sakarya, Turkey.

Funding

This study was supported by the Scientific Research Projects Commission of Sakarya University (Project No. 2009 50 02 005).

Notes

The authors declare no competing financial interest.

REFERENCES

(1) Kim, S.; Kim, H. J. Curing behavior and viscoelastic properties of pine and wattle tannin-based adhesives studied by dynamic mechanical thermal analysis and FT-IR-ATR spectroscopy. *J. Adhes. Sci. Technol.* **2003**, *17*, 1369−1383.

(2) Hesse, W. Phenolic Resins Wiesbaden. *Ullmann's Encyclopedia of Industrial Chemistry*; Wiley VCH: Germany; 2004.

(3) Hemingway, R. W.; Laks, P. E. *Plant Polyphenols*; Plenum Press: New York, 1992.

(4) Hamamoto, K.; Kawakita, H.; Ohto, K.; Inoue, K. Polymerization of phenol derivatives by the reduction of gold ions to gold metal. *React. Funct. Polym.* **2009**, *69*, 694−697.

(5) Alonso, M.; Oliet, M.; Dominguez, J.; Rojo, E.; Rodriguez, F. Thermal degradation of lignin-phenol-formaldehyde and phenol-formaldehyde resol resins. *J. Therm. Anal. Calorim.* **2011**, *105*, 349−356.

(6) Kim, S.; Kim, H. S.; Kim, H. J.; Yang, H. S. Fast curing PF resin mixed with various resins and accelerators for building composite materials. *Constr. Build. Mater.* **2008**, *22*, 2141−2146.

(7) Adams, B. A.; Holmes, E. L. Absorptive properties of synthetic resins: Part I. *J. Soc. Chem. Ind.* **1935**, *54*, 1T−9T.

(8) Malshe, V. C.; Sujatha, E. S. Phenol based resin as alkylation catalyst. *React. Funct. Polym.* **2000**, *43*, 183−194.

(9) Strelko, V.; Streat, M.; Kozynchenko, O. Preparation, characterisation and sorptive properties of polymer based phosphorus-containing carbon. *React. Funct. Polym.* **1999**, *41*, 245−253.

(10) Gorshkov, V. I.; Ivanov, V. A.; Staina, I. V. Selectivity of phenol−formaldehyde resins and separation of rare alkali metals. *React. Funct. Polym.* **1998**, *38*, 157−176.

(11) Santana, J. L.; Lima, L.; Torres, J.; Martínez, F.; Olivares, S. Simultaneous metal adsorption on tannin resins. *J. Radioanal. Nucl. Ch.* **2002**, *251*, 467−471.

(12) Inoue, K.; Kawakita, H.; Ohto, K.; Oshima, T. Adsorptive removal of uranium and thorium with a crosslinked persimmon peel gel. *J. Radioanal. Nucl. Chem.* **2006**, *267*, 435−442.

(13) Liao, X.; Ma, H.; Wang, R.; Shi, B. Adsorption of UO22+ on tannins immobilized collagen fiber membrane. *J. Membr. Sci.* **2004**, *243*, 235−241.

(14) Liao, X.; Li, L.; Shi, B. Adsorption recovery of thorium(IV) by Myrica rubra tannin and larch tannin immobilized onto collagen fibres. *J. Radioanal. Nucl. Ch.* **2004**, *260*, 619−625.

(15) Bulut, E.; Özacar, M. Rapid, Facile Synthesis of Silver Nanostructure Using Hydrolyzable Tannin. *Ind. Eng. Chem. Res.* **2009**, *48*, 5686−5690.

(16) Nakano, Y.; Ogata, T.; Kim, Y. H. Selective Recovery Process for Gold Utilizing a Functional Gel Derived from Natural Condensed Tannin. *J. Chem. Eng. Jpn.* **2007**, *40*, 270−274.

(17) Garro-Galvez, J. M.; Riedl, B. Pyrogallol-formaldehyde thermosetting adhesives. *J. Appl. Polym. Sci.* **1997**, *65*, 399−408.

(18) Wang, R.; Liao, X.; Shi, B. Adsorption Behaviors of Pt(II) and Pd(II) on Collagen Fiber Immobilized Bayberry Tannin. *Ind. Eng. Chem. Res.* **2005**, *44*, 4221−4226.

(19) Xiong, Y.; Adhikari, C. R.; Kawakita, H.; Ohto, K.; Inoue, K.; Harada, H. Selective recovery of precious metals by persimmon waste chemically modified with dimethylamine. *Bioresour. Technol.* **2009**, *100*, 4083−4089.

(20) Ma, H.; Liao, X.; Liu, X.; Shi, B. Recovery of platinum(IV) and palladium(II) by bayberry tannin immobilized collagen fiber membrane from water solution. *J. Membr. Sci.* **2006**, *278*, 373−380.

(21) Kawakita, H.; Hamamoto, K.; Ohto, K.; Inoue, K. Polyphenol Polymerization by Horseradish Peroxidase for Metal Adsorption Studies. *Ind. Eng. Chem. Res.* **2009**, *48*, 4440−4444.

(22) Uheida, A.; Iglesias, M.; Fontàs, C.; Hidalgo, M.; Salvadó, V. Sorption of palladium(II), rhodium(III), and platinum(IV) on Fe3O4 nanoparticles. *J. Colloid. Interface Sci.* **2006**, *301*, 402−408.

(23) Turner, A.; Crusell, M.; Millward, G. E.; Belo-Garcia, A.; Fisher, A. S. Adsorption Kinetics of Platinum Group Elements in River Water. *Environ. Sci. Technol.* **2006**, *40*, 1524−1531.

(24) Alam, M. S.; Inoue, K.; Yoshizuka, K.; Ishibashi, H. Adsorptive Separation of Rhodium(lll) Using Fe(Ill)-Templated Oxine Type of Chemically Modified Chitosan. *Sep. Sci. Technol.* **1998**, *33*, 655−666.

(25) Goto, M.; Kasaini, H.; Furusaki, S. Selective Separation of Pd(II), Rh(III), and Ru(III) Ions from a Mixed Chloride Solution Using Activated Carbon Pellets. *Sep. Sci. Technol.* **2000**, *35*, 1307−1327.

(26) Uheida, A.; Iglesias, M.; Fontàs, C.; Zhang, Y.; Muhammed, M. Adsorption Behavior of Platinum Group Metals (Pd, Pt, Rh) on Nonylthiourea-Coated Fe3O4 Nanoparticles. *Sep. Sci. Technol.* **2006**, *41*, 909−923.

(27) Holopainen, T.; Alvila, L.; Rainio, J.; Pakkanen, T. T. IR Spectroscopy as a Quantitative and Predictive Analysis Method of Phenol−Formaldehyde Resol Resins. *J. Appl. Polym. Sci.* **1998**, *69*, 2175−2185.

(28) Wang, W. J.; Perng, L. H.; Hsiue, G. H.; Chang, F. C. Characterization and properties of new silicone-containing epoxy resin. *Polymer* **2000**, *41*, 6113−6122.

(29) Wasikiewicz, J. M.; Mitomo, H.; Seko, N.; Tamada, M.; Yoshii, F. Platinum and palladium ions adsorption at the trace amounts by

radiation crosslinked carboxymethylchitin and carboxymethylchitosan hydrogels. *J. Appl. Polym. Sci.* **2007**, *104*, 4015−4023.
(30) Loyalka, S. K.; Riggs, C. A. Inverse Problem in Diffuse Reflectance Spectroscopy: Accuracy of the Kubelka-Munk Equations. *Appl. Spectrosc.* **1995**, *49* (8), 1107−1110.
(31) Barron, V.; Torrent, J. Use of the Kubelka-Munk theory to study the influence of iron oxides on soil colour. *J. Soil Sci.* **1986**, *37* (4), 499−510.
(32) Armaroli, T.; Bécue, T.; Gautier, S. Diffuse Reflection Infrared Spectroscopy (Drifts): Application to the in Situ Analysis of Catalysts. *Oil Gas Sci. Technol.* **2004**, *59* (2), 215−237.
(33) Poljanšek, I.; Krajnc, M. Characterization of Phenol-Formaldehyde Prepolymer Resins by In Line FT-IR Spectroscopy. *Acta Chim. Slov.* **2005**, *52*, 238−244.
(34) Handique, J.; Baruah, J. Polyphenolic compounds: an overview. *React. Funct. Polym.* **2002**, *52*, 163−188.
(35) Raquez, J.-M.; Deléglise, M.; Lacrampe, M.-F.; Krawczak, P. Thermosetting (bio)materials derived from renewable resources: A critical review. *Prog. Polym. Sci.* **2010**, *35*, 487−509.
(36) Peña, C.; Larrañaga, M.; Gabilondo, N.; Tejado, A.; Echeverria, J. M.; Mondragon, I. Synthesis and characterization of phenolic novolacs Modified by Chestnut and Mimosa Tannin Extracts. *J. Appl. Polym. Sci.* **2006**, *100*, 4412−4419.
(37) Mohammed-Ziegler, I.; Billes, F. Vibrational spectroscopic calculations on pyrogallol and gallic acid. *J. Mol. Struct.: THEOCHEM* **2002**, *618*, 259−265.
(38) Lee, Y. K.; Kim, H. J.; Rafailovich, M.; Sokolov, J. Curing monitoring of phenolic resol resins via atomic force microscope and contact angle. *Int. J. Adhes. Adhes.* **2002**, *22*, 375−384.
(39) Silverstein, R. M.; Webster, F. X. Infrared spectrometry. In *Spectrometric Identification of Organic Compounds*, 6th ed.; Wiley: New York, 1998; pp 90−138.
(40) Poljansek, I.; Sebenik, U.; Krajnc, M. Characterization of phenol-urea-formaldehyde resin by inline FTIR spectroscopy. *J. Appl. Polym. Sci.* **2006**, *99*, 2016−2028.
(41) Keresztury, G.; Billes, F.; Kubinyi, M.; Sundius, T. A. Density Functional, Infrared Linear Dichroism, and Normal Coordinate Study of Phenol and its Deuterated Derivatives: Revised Interpretation of the Vibrational Spectra. *J. Phys. Chem. A* **1998**, 1371−1380.
(42) Choi, M. H.; Byun, H. Y.; Chung, I. J. The effect of chain length of flexible diacid on morphology and mechanical property of modified phenolic resin. *Polymer* **2002**, *43* (16), 4437−4444.
(43) Arasaretnam, S.; Karunanayake, L. Synthesis, Characterization, and Metal Adsorption Properties of Tannin−Phenol−Formaldehyde Resins Produced Using Tannin from Dried Fruit of Terminalia chebula (Aralu). *J. Appl. Polym. Sci.* **2010**, *115*, 1081−1088.
(44) Özacar, M.; Soykan, C.; Şengil, İ. A. Studies on Synthesis, Characterization, and Metal Adsorption of Mimosa and Valonia Tannin Resins. *J. Appl. Polym. Sci.* **2006**, *102*, 786−797.
(45) Can, M. *Adsorption of Palladium and Rhodium onto Polyphenol-Formaldehyde Resins*, Ph.D. Thesis. Institute of Science and Technology, Sakarya University, Sakarya, Turkey, 2011.
(46) Gerber, W. J.; Koch, K. R.; Rohwer, H. E.; Hosten, E. C.; Geswindt, T. E. Separation and quantification of $[RhCl_n(H_2O)_{6-n}]_{3-n}$ (n = 0−6) complexes, including stereoisomers, by means of ion-pair HPLC−ICP-MS. *Talanta* **2010**, *85*, 348−358.
(47) Salvado, V.; Sanchez, J. M.; Hidalgo, M.; Havel, J. The speciation of rhodium(III) in hydrochloric acid media by capillary zone electrophoresis. *Talanta* **2002**, *56*, 1061−1071.
(48) Pletcher, D.; Urbina, R. I. Electrodeposition of rhodium. Part 1. Chloride solutions. *J. Electroanal. Chem.* **1997**, *42*, 137−144.
(49) Piron, E.; Accominotti, M.; Domard, A. Interaction between Chitosan and Uranyl Ions. Role of Physical and Physicochemical Parameters on the Kinetics of Sorption. *Langmuir* **1997**, *13*, 1653−1658.
(50) Aleksenko, S. S.; Gumenyuk, A. P.; Mushtakova, S. P.; Timerbaev, A. R. Speciation studies by capillary electrophoresis−distribution of rhodium(III) complexed forms in acidic media. *Fresenius J. Anal. Chem.* **2001**, *370*, 865−871.
(51) Huang, X.; Wang, Y.; Liao, X.; Shi, B. Adsorptive recovery of Au^{3+} from aqueous solutions using bayberry tannin-immobilized mesoporous silica. *J. Hazard. Mater.* **2010**, *183*, 793−798.
(52) Jaén, J. A.; González, L.; Vargas, A.; Olave, G. Gallic Acid, Ellagic Acid and Pyrogallol Reaction with metallic iron. *Hyperfine Interact.* **2003**, *148/149*, 227−235.
(53) Vanỳsek, P. Electrochemical Series. In *CRC Handbook of Chemistry and Physics*; CRC Press: Boca Raton, 2005; pp 8−20.
(54) Nematollahi, D.; Rafiee, M. Electrochemical oxidation of catechols in the presence of acetylacetone. *J. Electroanal. Chem.* **2004**, *566*, 31−37.
(55) Parajuli, D.; Kawakita, H.; Inoue, K.; Ohto, K.; Kajiyama, K. Persimmon peel gel for the selective recovery of gold. *Hydrometallurgy* **2007**, *87*, 133−139.
(56) Kawakita, H.; Yamauchi, R.; Parajuli, D.; Ohto, K.; Harada, H.; Inoue, K. Recovery of Gold from Hydrochloric Acid by means of Selective Coagulation with Persimmon Extract. *Sep. Sci. Technol.* **2008**, *43*, 2375−2385.

NOTE ADDED AFTER ASAP PUBLICATION

This paper was published on the Web on September 18, 2012, with incorrect text in the abstract. The corrected version was reposted on September 19, 2012.